

1

2 Observational constraints on the chemistry of isoprene

3 nitrates over the eastern United States

4

5

6

7 Larry W. Horowitz, Arlene M. Fiore, and George P. Milly

8 NOAA Geophysical Fluid Dynamics Laboratory, Princeton, NJ

9

10 Ronald C. Cohen, Anne Perring, and Paul J. Wooldridge

11 Department of Chemistry, UC Berkeley, Berkeley , CA

12

13 Peter G. Hess, Louisa K. Emmons, Jean-François Lamarque

14 Atmospheric Chemistry Division, National Center for Atmospheric Research, Boulder, CO

15

16

17 *Journal of Geophysical Research*

18 Submitted July 3, 2006

19 First revision and resubmission, October 2006

20 Second revision and resubmission, January 2007

Abstract

The formation of organic nitrates during the oxidation of the biogenic hydrocarbon isoprene can strongly affect boundary layer concentrations of ozone and nitrogen oxides ($\text{NO}_x = \text{NO} + \text{NO}_2$). We constrain uncertainties in the chemistry of these isoprene nitrates using chemical transport model simulations in conjunction with observations over the eastern United States from the International Consortium for Atmospheric Research on Transport and Transformation (ICARTT) field campaign during summer 2004. The model best captures the observed boundary layer concentrations of organic nitrates and their correlation with ozone using: a 4% yield of isoprene nitrate production from the reaction of isoprene hydroxyperoxy radicals with NO, a recycling of 40% NO_x when isoprene nitrates react with OH and ozone, and a fast dry deposition rate of isoprene nitrates. Simulated boundary layer concentrations are only weakly sensitive to the rate of photochemical loss of the isoprene nitrates. An 8% yield of isoprene nitrates degrades agreement with the observations somewhat, but concentrations are still within 50% of observations and thus cannot be ruled out by this study. Our results indicate that complete recycling of NO_x from the reactions of isoprene nitrates and slow rates of isoprene nitrate deposition are incompatible with the observations. We find that ~50% of the isoprene nitrate production in the model occurs via reactions of isoprene (or its oxidation products) with the NO_3 radical, but note that the isoprene nitrate yield from this pathway is highly uncertain. Using recent estimates of rapid reaction with ozone, 20-24% of isoprene nitrates are lost via this pathway, implying that ozonolysis is an important loss process for isoprene nitrates. Isoprene nitrates are shown to have a major impact on the nitrogen oxide ($\text{NO}_x = \text{NO} + \text{NO}_2$) budget in the summertime U.S. continental boundary layer, consuming 15-19% of the emitted NO_x , of which 4-6% is recycled back to NO_x and the remainder is exported as isoprene nitrates (2-3%) or

1 deposited (8-10%). Our constraints on reaction rates, branching ratios, and deposition rates need
2 to be confirmed through further laboratory and field measurements. The model systematically
3 underestimates free tropospheric concentrations of organic nitrates, indicating a need for future
4 investigation of the processes controlling the observed distribution.

1. Introduction

Photochemical oxidation of volatile organic compounds (VOCs) in the presence of nitrogen oxides ($\text{NO}_x = \text{NO} + \text{NO}_2$) contributes to the production of ozone. Over the eastern United States during summer, chemical reactivity and subsequent ozone production are dominated by isoprene (2-methyl-1,3-butadiene), an abundant biogenic VOC that reacts rapidly with OH [e.g., *Trainer et al.*, 1987]. Isoprene oxidation also modulates the partitioning and fate of reactive nitrogen within the continental boundary layer [e.g., *Horowitz et al.*, 1998; *Houweling et al.*, 1998].

Recent modeling studies have demonstrated that ozone concentrations and reactive nitrogen partitioning are sensitive to uncertainties in the isoprene chemical oxidation pathways [*Horowitz et al.*, 1998; *von Kuhlmann et al.*, 2004; *Fiore et al.*, 2005; *Wu et al.*, 2007]. Specific uncertainties include the magnitude and spatial distribution of isoprene emissions, the yield and fate of isoprene nitrates, and the fate of organic hydroperoxides. Previous studies suggest that surface ozone is only weakly sensitive to the uncertainties in organic hydroperoxides (up to 2-3 ppbv), while the choice of isoprene emissions inventory can have large local or regional effects (up to 15 ppbv ozone locally) [*von Kuhlmann et al.*, 2004; *Fiore et al.*, 2005]. We focus on the uncertainties in isoprene nitrate chemistry, which have been shown to affect surface ozone (by up to 10 ppbv) and NO_x (by up to 10%) [*Horowitz et al.*, 1998; *von Kuhlmann et al.*, 2004; *Fiore et al.*, 2005]. We analyze chemical transport model simulations in conjunction with observations from the International Consortium for Atmospheric Research on Transport and Transformation (ICARTT) field campaign [*Fehsenfeld et al.*, 2006; *Singh et al.*, 2006] conducted in summer

2004 to constrain the uncertainties in isoprene nitrate chemistry and examine the implications of these constraints for the NO_x budget and ozone concentrations over the eastern United States.

When isoprene is oxidized by OH, six different isomeric hydroxyperoxy (RO₂) radicals are formed (after the addition of O₂). Under high-NO_x conditions these radicals typically react with NO, forming primarily hydroxalkoxy (RO) radicals with a minor channel leading to the production of organic hydroxynitrates (RONO₂, “isoprene nitrates”) [e.g., *Chen et al.*, 1998]. Laboratory studies have estimated the yield of isoprene nitrates from the RO₂+NO reaction to range from 4.4% to 15% [*Chen et al.*, 1998; *Tuazon and Atkinson*, 1990 (corrected as discussed by *Paulson et al.*, 1992); *Chuong and Stevens*, 2002; *Sprengnether et al.*, 2002]. Model studies have shown that tropospheric ozone production and surface concentrations are sensitive to the isoprene nitrate yield [*von Kuhlmann et al.*, 2004; *Wu et al.*, 2007].

The oxidation of isoprene by NO₃, which occurs primarily at night, leads to the production of another set of isoprene nitrates. This pathway proceeds by addition of NO₃ to one of the double bonds in isoprene followed by addition of O₂ to form nitrooxyalkyl peroxy radicals. These radicals can then either undergo subsequent reactions to form stable organic nitrates or decompose to release NO_x; the relative amounts of organic nitrates versus released NO_x are poorly known [e.g., *Paulson and Seinfeld*, 1992; *Fan and Zhang*, 2004]. The isoprene nitrates formed by the isoprene-NO₃ channel are expected to be aldehydic [*Paulson and Seinfeld*, 1992] or ketonic nitrates [*Fan and Zhang*, 2004], as opposed to the hydroxynitrates formed from the isoprene-OH channel. The importance of the NO₃ versus OH pathways for isoprene nitrate production is also uncertain, but modeling [*von Kuhlmann et al.*, 2004] and observational [*Starn*

1 *et al.*, 1998] studies both suggests that the isoprene-NO₃ channel may be a major source of
2 isoprene nitrates.

3
4 Isoprene nitrates contain a double bond, so they are highly reactive towards OH, ozone,
5 and NO₃. Reaction with OH is expected to be the major chemical loss. Estimates of the reaction
6 rate constant for isoprene nitrates + OH range from (1.3-9)x10⁻¹¹ molec⁻¹ cm³ s⁻¹ [*Paulson and*
7 *Seinfeld*, 1992; *Shepson et al.*, 1996, *Chen et al.*, 1998; *Giacopelli et al.*, 2005], although some
8 model studies have assumed rate constants as low as 6.8x10⁻¹³ [*Brasseur et al.*, 1998]. *Giacopelli*
9 *et al.* [2005] estimate a rate constant for isoprene nitrates + ozone of 1.33x10⁻¹⁷ for terminally
10 double-bonded isomers and a much faster rate constant of 4.03x10⁻¹⁶ for internally double-
11 bonded isomers, based on previous estimates for structurally similar alkenes. These rate
12 constants correspond to a wide range in the lifetime of isoprene nitrates versus reaction with
13 ozone (at 40 ppb ozone), from ~40 min. (for internally double-bonded isomers) to ~20 hours (for
14 terminally bonded isomers). Previous modeling studies have used rate constants as low as
15 2.25x10⁻¹⁸ based on the rate constants for methylvinyl ketone and methacrolein [e.g., *Horowitz et*
16 *al.*, 1998], or neglected this reaction entirely [e.g., *Pöschl et al.*, 2000].

17
18 The products of the isoprene nitrate chemical reactions have not been directly measured.
19 *Paulson and Seinfeld* [1992] suggested that reaction with OH should release NO_x, while other
20 studies conclude that the reaction of some isomers will lead to the production of secondary
21 multifunctional organic nitrates [*Grossenbacher et al.*, 2001; *Giacopelli et al.*, 2005]. The release
22 of NO_x by this reaction or its continued sequestration in organic nitrates can significantly alter
23 the extent to which isoprene chemistry acts as a sink for NO_x [e.g., *Chen et al.*, 1998; *Horowitz*

1 *et al.*, 1998], with up to ~10% effects on surface ozone concentrations [*von Kuhlmann et al.*,
2 2004; *Fiore et al.*, 2005]. The efficiency of NO_x recycling from the reactions of isoprene nitrates
3 with ozone and NO₃ is also poorly known.

4
5 Removal of isoprene nitrates by wet and dry deposition provides a permanent sink for
6 atmospheric NO_x. The rate of wet deposition depends on the Henry's law constant, which has
7 been estimated by analogy with comparable species to range from $H(298K) = 6.0 \times 10^3 \text{ M atm}^{-1}$
8 [*Shepson et al.*, 1996] to 1.7×10^4 [*von Kuhlmann et al.*, 2004]. Estimates of the dry deposition
9 velocity of isoprene nitrates range from that of PAN (0.4-0.65 cm s⁻¹) [*Shepson et al.*, 1996;
10 *Giacopelli et al.*, 2005] to that of HNO₃ (4-5 cm s⁻¹) [*Rosen et al.*, 2004; *Horii et al.*, 2006].
11 Using the slower deposition estimates and an OH rate constant of $1.3 \times 10^{-11} \text{ molec}^{-1} \text{ cm}^3 \text{ s}^{-1}$,
12 *Shepson et al.* [1996] predicted that reaction with OH should dominate over deposition, yielding
13 overall atmospheric lifetime of ~18h (note that the reaction of isoprene nitrates with ozone was
14 neglected in that study).

15
16 The ICARTT multi-agency international field campaign conducted during summer 2004
17 included measurements of isoprene, its oxidation products, reactive nitrogen compounds, and
18 ozone over the eastern United States. Since chemistry in this region and season is strongly
19 influenced by emissions of both biogenic isoprene and anthropogenic NO_x, the ICARTT
20 campaign presents an opportunity to study the effect of isoprene on reactive nitrogen partitioning
21 and ozone production. We analyze the ICARTT observations in conjunction with a 3-
22 dimensional chemical transport model to identify new constraints on the chemistry of isoprene
23 nitrates. The model is described in Section 2, and evaluated with observations in Section 3. In

Section 4, we examine the sensitivity of our results to uncertainties in isoprene nitrate chemistry, derive observational constraints on this chemistry, and discuss the implications for the NO_x budget over the eastern United States. Conclusions are presented in Section 5.

2. Model description

We simulate the chemistry during the ICARTT period (July-August 2004) using the Model of Ozone and Related Chemical Tracers, version 4 (MOZART-4) chemical transport model [Emmons *et al.*, 2006, manuscript in preparation]. This model is an updated version of the MOZART-2 model [Horowitz *et al.*, 2003] with aerosol chemistry based on that of Tie *et al.* [2005]. In MOZART-4, photolysis rates are calculated interactively to account for absorption and scattering by aerosols and clouds with Fast-TUV [Madronich and Flocke, 1998; Tie *et al.*, 2005]. The influx of O₃ from the stratosphere is prescribed using the SYNOZ technique (500 Tg yr⁻¹) [McLinden *et al.*, 2000]. The prescribed monthly mean deposition velocities for O₃ and PAN have been increased based on those used by Bey *et al.* [2001], although a recent observational study suggests that the PAN deposition velocities may still be underestimated [Turnipseed *et al.*, 2006]. The mechanism now represents the chemistry of higher alkanes with the “bigalk” (C₅H₁₂) tracer, a lumped species representing the butanes, pentanes, and hexanes. Higher alkenes are included as “bigene” (C₄H₈), a lumped species representing mostly 2-methylpropene and 2-butene. An additional new species, “toluene” (C₇H₈), is a lumped aromatic compound representing mostly benzene, toluene, and the xylenes. Additional oxidation products of the above species have also been added. Updates to the chemistry in MOZART-4 are more fully described by Emmons *et al.* [2006].

1
2 The isoprene and monoterpene oxidation mechanisms in our BASE simulation are shown
3 in Table 1. In Section 4, we evaluate the sensitivity of our results to the assumptions in our
4 BASE isoprene mechanism described here, using the additional model simulations described in
5 Table 2. The treatment of isoprene nitrates has been modified from that in MOZART-2
6 [Horowitz *et al.*, 2003]. The yield of ONITR from the addition branch of the ISOP₂ + NO
7 reaction has been decreased from 8% in MOZART-2 to 4% [e.g., Chen *et al.*, 1998] in the BASE
8 simulation. A new species (XNITR in Table 1) represents secondary multifunctional organic
9 nitrates. The reaction of primary isoprene nitrates (ONITR) with OH recycles 40% of NO_x,
10 rather than 100% as in MOZART-2, with the balance forming XNITR based on recent studies
11 suggesting that this reaction produces some secondary nitrates [e.g., Grossenbacher *et al.*, 2001;
12 Giacomelli *et al.*, 2005]. XNITR is removed by wet and dry deposition at the same rates as
13 ONITR, but has no chemical losses in our mechanism, as its further reactions are assumed to
14 convert it to more highly substituted organic nitrates. The reaction ONITR + ozone has been
15 added with a reaction rate constant based on a weighted average of the values recommended by
16 Giacomelli *et al.* [2005], with the same products as the ONITR + OH reaction. The reaction
17 ONITR + NO₃ is also assumed to produce XNITR. Note that the carbonyl nitrates produced from
18 the isoprene-NO₃ channel (via ISOPNO₃) are represented in our mechanism by the same ONITR
19 species as the hydroxynitrates from the isoprene-OH channel. This simplifying assumption
20 neglects any differences in reactivity or deposition between these two different classes of
21 isoprene nitrates.

1 The oxidation scheme for monoterpenes, represented by α -pinene, has been updated to
2 reflect recent laboratory data (see Table 1 and *Emmons et al.* [2006]). We assume that terpene
3 oxidation produces organic nitrates with an 18% yield from the reaction of terpene peroxy
4 radicals (TERPO₂) with NO, based on estimates by *Nozière et al.* [1999]. We note that this yield
5 is considerably higher than the ~1% yield estimated by *Aschmann et al.* [2002], although
6 *Aschmann et al.* acknowledged the possibility that their results were biased low by aerosol
7 formation or loss to the chamber wall.

8
9 Global emissions were specified as by *Horowitz et al.* [2003], with anthropogenic
10 emissions based on EDGAR v2.0 [*Olivier et al.*, 1996] and biomass burning from *Müller* [1992]
11 and *Hao and Liu* [1994] with emission ratios from *Andreae and Merlet* [2001]. Isoprene and
12 monoterpene emissions are calculated interactively based on temperature, sunlight, and
13 vegetation type using algorithms from the Model of Emissions of Gases and Aerosols from
14 Nature (MEGAN v.0) [*Guenther et al.*, 2006]. Over North America during summer, we use
15 updated anthropogenic surface emissions based on the EPA National Emissions Inventory
16 (NEI99, version 3, <http://www.epa.gov/ttn/chief/net/1999inventory.html>) [S. McKeen, personal
17 communication, 2004], and the daily biomass burning emission inventory developed by *Turquety*
18 *et al.* [2007]. Biomass burning emissions are distributed vertically up to 4 km altitude, with 70%
19 of the emissions occurring below 2 km. Surface emissions over the eastern United States (24-
20 52°N, 62.5-97.5°W) in July 2004 total 0.52 TgN NO_x, 7.8 Tg CO, 3.7 TgC isoprene, and 0.91
21 TgC terpenes.

1 Meteorological fields are provided by the NCEP Global Forecast System (GFS) every
2 three hours. The model resolution is 1.9° latitude x 1.9° longitude, with 64 vertical levels, and a
3 dynamical and chemical timestep of 15 minutes. The BASE model simulation was conducted
4 from December 2003 through the ICARTT period (July-August 2004). Sensitivity simulations
5 (Section 4.1) begin in May 2004, allowing for a two-month spinup period sufficient to capture
6 changes in summertime continental boundary layer chemistry.

8 **3. Results from base simulation**

10 **3.1 Evaluation with ICARTT observations**

12 We evaluate the results of the MOZART-4 BASE simulation with observations made on
13 board the NASA DC-8 [*Singh et al.*, 2006] and NOAA WP-3D [*Fehsenfeld et al.*, 2006] aircraft
14 during ICARTT. Simulated concentrations are sampled every minute along the flight tracks of
15 the two aircraft and then averaged onto the model grid for each flight. The two aircraft pursued
16 different sampling strategies: the DC-8, based in St. Louis, Missouri and Portsmouth, New
17 Hampshire, typically aimed to sample regionally representative air masses; the WP-3D, based in
18 Portsmouth, New Hampshire often sampled local plumes from urban outflow or power plants.
19 (See ICARTT overview papers [*Fehsenfeld et al.*, 2006; *Singh et al.*, 2006] for more details
20 about the aircraft flight tracks.)

Comparisons of selected species, including isoprene, isoprene oxidation products, ozone, and ozone precursors, below 2km in the eastern United States are presented in Figure 1. Isoprene concentrations show little bias, but are poorly correlated with observations ($r^2 = 0.09$ and mean bias = +14% for NASA, $r^2 = 0.31$ and bias = -17% for NOAA), most likely due to the short lifetime of isoprene and the high spatial variability of its emissions. The first generation isoprene oxidation products methylvinyl ketone and methacrolein, which have longer atmospheric lifetimes, are better simulated by the model ($r^2 = 0.50$, bias = -11%). Monoterpene concentrations are underestimated by almost a factor of 2, but correlated with observations ($r^2 = 0.33$). Overall, we conclude that the MEGAN biogenic emission inventory captures the magnitude and large-scale spatial pattern of isoprene emissions, but may underestimate terpene emissions.

Boundary-layer concentrations of ozone are slightly overestimated (mean bias = +6.5% for NASA, +2.4% for NOAA) and moderately correlated with observations ($r^2 = 0.31$ for NASA, 0.17 for NOAA). CO and NO_x are moderately well correlated with observations ($r^2 = 0.43$ and 0.12 for CO from NASA and NOAA, respectively, $r^2 = 0.36$ for NO_x from NASA), with an average model overestimate of ~15% for CO and ~30% for NO_x. The model overestimate of NO_x concentrations can be attributed to our use of the NEI99 emission inventory (for the year 1999), which overestimates the power-plant emissions of NO_x during 2004 [Frost *et al.*, 2006]. The lower correlations of our results with the NOAA measurements are expected as a result of the poor representation of the local plumes sampled by the WP-3D in our coarse resolution model. Secondary oxidation products PAN and formaldehyde (CH₂O) are well correlated with the observations, but PAN tends to be overestimated in the boundary layer. PAN concentrations

1 in the free troposphere have little mean bias (not shown). Simulated organic nitrates (ONITR +
2 XNITR + ISOPNO₃ + other organic nitrates) are overestimated in the mean (+20%) versus the
3 observed total alkyl- and hydroxyalkyl-nitrates (Σ ANs) [Day *et al.*, 2002] (bias = +20%) and are
4 poorly correlated with the observations ($r^2=0.20$). We found little systematic correlation between
5 the errors in organic nitrates and those in the other species in Figure 1 (e.g., isoprene, NO_x, PAN,
6 CO). The small-scale errors in isoprene emissions mentioned above may contribute to errors in
7 the organic nitrates on the same scales, since isoprene is the major source of these nitrates
8 (Section 3.2). Concentrations of HNO₃ and H₂O₂ are poorly correlated with observations,
9 suggesting possible model errors in wet deposition.

10
11 With the exception of organic nitrates, the agreement between simulated and observed
12 concentrations for the species evaluated in Figure 1 is relatively insensitive to assumptions about
13 isoprene nitrate chemistry (at least to within model biases), as represented by the sensitivity
14 simulations in Section 4.1. We thus use only the observed Σ AN concentrations to provide
15 constraints on the chemistry of isoprene nitrates (Section 4.2). We begin by examining the
16 budget of isoprene nitrates in Section 3.2.

17 18 **3.2 Isoprene nitrate budget**

19
20 Budgets for isoprene nitrate (ONITR+XNITR) production and loss in the eastern United
21 States (24-52°N, 62.5-97.5°W) boundary layer (below 800 hPa) during July 2004 are presented
22 in Figure 2. In the BASE simulation, half of the isoprene nitrate production occurs through the
23 NO₃ pathway, in which isoprene reacts with NO₃ to form ISOPNO₃, which can then react with

NO, NO₃, or HO₂ to form carbonyl nitrates. These carbonyl nitrates, represented in our mechanism by the same ONITR species as the hydroxynitrates formed from the isoprene-OH pathway, are assumed to form with a yield of 79.4% from all ISOPNO₃ reaction pathways (see Table 1) [Horowitz *et al.*, 2003]. The large contribution of this pathway to isoprene nitrate production, despite the small fraction of isoprene oxidized via this pathway (~6%), agrees well with the findings of von Kuhlmann *et al.* [2004]. About 25% of the isoprene nitrate production occurs via the reaction ISOPO₂ + NO, which produces ONITR with a 4% yield in this simulation. Each of the reactions MACRO₂+NO and TERPO₂+NO (TERPO₂ is formed by terpenes+OH or terpenes+NO₃) yields another 12-14%. This partitioning of organic nitrate sources is similar to that calculated by Cleary *et al.* [2005] for the suburbs of Sacramento, CA. Note that we assume the same ONITR yield from terpenes+OH and terpenes+NO₃ (18%), while in the case of isoprene we include a much higher yield from isoprene+NO₃ (79.4%) than for isoprene+OH (4% in the BASE case); the actual yield of organic nitrates from terpenes+NO₃ is likely to be considerably higher than the 18% yield assumed in our mechanism. The loss of isoprene nitrates in the BASE simulation occurs largely by dry deposition (44%) and reaction with ozone (24%) and OH (10%), with additional losses by transport (16%) and wet deposition (5%).

4. Isoprene nitrate sensitivity analysis

In this section, we examine the sensitivity of our model results to assumptions concerning the production and loss of isoprene nitrates, using the additional simulations in Table 2. In particular, we examine the sensitivity of isoprene nitrates to the assumed yield, OH reaction rate,

recycling of NO_x, and deposition rate. We place constraints on the isoprene nitrate chemistry based on boundary layer observations of ΣAN, and quantify the effects of isoprene nitrates on the NO_x budget over the eastern United States.

4.1 Sensitivity simulations

The production of isoprene nitrates following the oxidation of isoprene by OH depends on the yield of these nitrates from the reaction of the isoprene peroxy radicals (ISOPO₂ in Table 1) with NO. We conduct sensitivity simulations in which the yield is increased from the BASE case value of 4% [Chen *et al.*, 1998] to 8%, as assumed by Fan and Zhang [2004]. In the simulations with an 8% yield (8% and 8%_slowCHEM in Table 2), the production of isoprene nitrates via the ISOPO₂+NO pathway doubles compared to the runs with a 4% yield (BASE and 4%_slowCHEM), but production via other pathways is relatively unchanged (Figure 2). Thus, the total production of isoprene nitrates increases by 23% in these simulations.

The chemical loss of isoprene nitrates (ONITR) is primarily through reaction with ozone (~70% in the BASE case), followed by reaction with OH. We test here the effects of slower photochemical loss of isoprene nitrates, as applied in earlier studies. Our BASE simulation assumes a rate constant of $k = 4.5 \times 10^{-11} \text{ molec}^{-1} \text{ cm}^3 \text{ s}^{-1}$ for isoprene nitrates + OH [Emmons *et al.*, 2006], within the range of $(3-9) \times 10^{-11} \text{ molec}^{-1} \text{ cm}^3 \text{ s}^{-1}$ estimated by Giacomelli *et al.* [2005] using the method of Kwok and Atkinson [1995]. There is evidence that the Kwok and Atkinson [1995] method may overestimate the rate constant for OH reaction with hydroxyalkyl nitrates by a factor of 2-21 [Neeb, 2000; Treves and Rudich, 2003], so we also consider a lower rate

constant of $k = 1.3 \times 10^{-11} \text{ molec}^{-1} \text{ cm}^3 \text{ s}^{-1}$ (simulations 4%_slowCHEM, 8%_slowCHEM), similar to that used in several other studies [Shepson *et al.*, 1996; Chen *et al.*, 1998; Pöschl *et al.*, 2000; Horowitz *et al.*, 2003]. In these simulations, we also decrease the rate of the isoprene nitrates + ozone reaction by a factor of 3 from its BASE case value of $k = 1.30 \times 10^{-16}$ and decrease the photolysis rate for ONITR, $J(\text{ONITR})$, from its BASE case value of $J(\text{CH}_3\text{CHO})$ to $J(\text{HNO}_3)$. The ONITR reactions with ozone and OH together account for 34% of the isoprene nitrate loss when a fast reaction rate is assumed (BASE and 8%), but only 29% when a slower rate is used (4%_slowCHEM and 8%_slowCHEM in Figure 2). Photolysis of ONITR is a minor loss in all simulations, accounting for 1% or less of the isoprene nitrate loss in all simulations. The overall lifetime of isoprene nitrates (ONITR+XNITR+ISOPNO₃) increases by only 5% in the simulations with slower ONITR photochemical loss (Table 2).

When isoprene nitrates (ONITR) react with ozone and OH, the reactive nitrogen can be recycled to NO_x or retained as XNITR. In the BASE case, we assume a NO_x recycling efficiency of 40%. Since this recycling efficiency is uncertain [Paulson and Seinfeld, 1992; Chen *et al.*, 1998; Grossenbacher *et al.*, 2001, Giacomelli *et al.*, 2005], we include three sensitivity simulations in which the recycling is varied from extreme values of 0% (4%_0%NO_x in Table 2) to 100% (4%_100%NO_x and 8%_slowCHEM_100%NO_x). When the recycling is completely turned off, the ONITR reactions with ozone and OH cease to be sinks for isoprene nitrates and instead produce 100% XNITR. As a result, the burden of isoprene nitrates increases by 56% (Table 2) and losses via dry and wet deposition increase by 43% and 60%, respectively (Figure 2). When the recycling is increased from 40% to 100%, the losses of isoprene nitrates from the ONITR reactions with ozone and OH increase nearly proportionally by a factor of 2.6 to account

1 together for 73-85% of the total loss, causing the isoprene nitrate burden and lifetime to decrease
2 by a factor of 5-12.

3
4 The final sensitivity we examine is the rate at which isoprene nitrates (ONITR and
5 XNITR) are lost by deposition. In the BASE simulation, we assume that isoprene nitrates deposit
6 rapidly, with a dry deposition velocity equal to that of HNO_3 and a wet deposition rate (Henry's
7 Law constant of $\text{H}_{298} = 7.51 \times 10^3 \text{ M atm}^{-1}$) similar to that assumed by *Shepson et al.* [1996].
8 Since dry deposition dominates over wet deposition as a loss pathway from the boundary layer
9 (see Section 3.2 and Figure 2), we examine the sensitivity of our results to the removal rate by
10 decreasing the dry deposition velocity of isoprene nitrates by a factor of ~20 to that of PAN
11 (simulations 4%_slowDD, 8%_slowDD) [*Shepson et al.*, 1996; *Giacopelli et al.*, 2005]. In these
12 simulations with slow dry deposition, the isoprene nitrate burden and lifetime increase by a
13 factor of 2 (Table 2) and export and chemical loss of ONITR by increase in importance,
14 accounting for 43% and 38% of the total loss, respectively (Figure 2).

16 **4.2 Constraints from observations**

17
18 The sensitivity simulations described above (Section 4.1 and Table 2) most dramatically
19 affect the concentrations of isoprene nitrates, with only small impacts on the other species
20 evaluated in Section 3.1. Previous calculations have shown that biogenically derived nitrates are
21 the primary source of ΣANs in Sacramento [*Cleary et al.*, 2005], in eastern Pennsylvania
22 [*Trainer et al.*, 1991], rural Michigan and Alabama [*Sillman and Samson*, 1995], and rural
23 Ontario [*O'Brien et al.*, 1995], but not in Houston, Texas [*Rosen et al.*, 2004] The speciated

(non-isoprene) alkyl nitrates measured from whole-air samples during ICARTT (by D. Blake) typically account for an average of only ~10% of the observed Σ ANs, indicating that the Σ ANs are primarily composed of larger compounds or multi-functional compounds such as the isoprene and terpene nitrates, consistent with the model results. A more detailed discussion of the comparison of individually measured nitrates to the observations of Σ ANs is presented in a forthcoming paper by A. Perring et al. (manuscript in preparation). In this section, we utilize measurements of total alkyl- and hydroxyalkyl-nitrates (Σ ANs) [Day et al., 2002] during ICARTT to constrain the chemistry of isoprene nitrates.

Simulated organic nitrate concentrations (ONITR + XNITR + ISOPNO₃ + other organic nitrates) are compared with observations of Σ ANs in Figure 3. The mean organic nitrates simulated in the BASE case agree well with observed concentrations in the boundary layer, with a bias of +10-20%, whereas a small negative bias may have been expected based on the previously discussed underestimate of MVK+MACR (Figure 1). The model underestimates free tropospheric Σ AN by about a factor of 3. The correlation of ozone with Σ ANs provides an additional means of evaluating organic nitrate abundances because both organic nitrates and ozone are produced from the reactions of RO₂ radicals with NO, so the concentration ratio may normalize for any model errors in the absolute concentrations of RO₂ or in the rate of boundary layer ventilation. The BASE model reproduces the observed Δ O₃/ Δ Σ AN correlation slope (81.0 simulated, 81.7 observed), although the correlation is much stronger in the model (r^2 =0.76 vs. 0.12 observed). This slope is similar to the relationship reported by Day et al. [2003] for a rural location in California and to those reported by Rosen et al. [2004] and Cleary et al. [2005] for urban areas in late afternoon. Based on the methodology of Rosen et al. [2004] and Cleary et al.

1 [2005], a $\Delta\text{O}_3/\Delta\Sigma\text{AN}$ slope of 81.7 corresponds to an “effective ΣAN yield” of 2.4% from the
2 complete mix of ozone-producing VOCs. An “effective ΣAN yield” of about a factor of two
3 lower than the yield calculated from OH-initiated VOC chemistry (dominated here by isoprene)
4 in the daytime is similar to results reported by *Rosen et al.* [2004] and *Cleary et al.* [2005]. The
5 8% simulation overestimates ΣANs (+40% bias) and underestimates the $\Delta\text{O}_3/\Delta\Sigma\text{AN}$ slope (62.8).

6
7 The simulations with slower photochemical loss of ONITR (4%_slowCHEM and
8 8%_slowCHEM) have only slightly (+5-6%) higher boundary layer concentrations (Figure 3)
9 and burdens (Table 2) of ΣANs than the corresponding simulations with the faster ONITR+OH
10 reaction rate, even though the ozone and OH reaction rate constants were decreased by about a
11 factor of 3. This small response reflects the much larger contribution to ΣANs from secondary
12 multifunctional nitrates (XNITR, accounting for 92% of ΣANs in BASE) than from primary
13 isoprene nitrates (ONITR). In the 4%_slowCHEM simulation, the burden of ONITR (which has
14 photochemical losses) increases by a factor of 2.5 versus BASE, but XNITR (which is produced
15 from ONITR, but lost only by export and deposition) decreases by -7.4%. The higher
16 concentrations of ΣANs decrease the $\Delta\text{O}_3/\Delta\Sigma\text{AN}$ correlation slope slightly, with little impact on
17 mean concentrations (Figure 3).

18
19 When the reactions of ONITR with ozone and OH are allowed to recycle all of the NO_x
20 (4%-100% NO_x), boundary layer concentrations of ΣAN are underestimated by a factor of 6 or
21 more. If we additionally assume an 8% yield of ONITR and slow photochemical loss, the ΣAN
22 concentrations increase, but are still a factor of 2.5-4 below observed values, and the $\Delta\text{O}_3/\Delta\Sigma\text{AN}$
23 correlation slope is still greatly overestimated (252.0). In both of the simulations with 100%

1 recycling (4%_100%NO_x, 8%_slowCHEM_100%_NO_x), free tropospheric ΣAN concentrations
2 are dramatically underestimated by a factor of 15 or more. On the other hand, if the ONITR
3 reactions with OH and ozone are assumed to recycle no NO_x (4%_0%NO_x), instead forming
4 XNITR exclusively, ΣAN concentrations increase by over 50% from the BASE case, leading to
5 70% overestimates of observed boundary layer ΣAN and a large underestimate of ΔO₃/ΔΣAN
6 (50.7).
7

8 In the final set of sensitivity simulation, the dry deposition velocity of isoprene nitrates is
9 decreased from that of HNO₃ to that of PAN (simulations 4%_slowDD and 8%_slowDD). In
10 these simulations, ΣAN concentrations increase by approximately a factor of 2, dramatically
11 worsening agreement with observed ΣAN concentrations and ΔO₃/ΔΣAN correlation slopes in
12 the boundary layer; simulated concentrations of ΣAN in the free troposphere approach observed
13 values, but are still slightly underestimated. The discrepancy between simulated and observed
14 ΣAN in the free troposphere is discussed further below.
15

16 Based on the comparisons with observed boundary-layer ΣANs and ΔO₃/ΔΣAN, we find
17 that the BASE and 4%_slowCHEM simulations — with a 4% yield of isoprene nitrates from
18 ISOPO₂+NO, recycling of 40% NO_x, and fast loss by dry deposition — best match observations
19 of ΣAN concentrations and ΔO₃/ΔΣAN correlation slopes. The simulations with an 8% yield
20 degrade agreement with observation somewhat. The simulations with slow dry deposition and
21 those with either 0% or 100% NO_x recycling show the worst agreement with observations. Based
22 on these results, we select the BASE and 4%_slowCHEM cases as the “best guess” set of model

1 parameters, but also consider a range of uncertainty including the other simulations showing
2 reasonable agreement (within $\sim\pm 50\%$) with observations (8%, 8%_slowCHEM).

3
4 Our best guess of a 4% yield of isoprene nitrates agrees well with the values measured by
5 *Chen et al.* [1998], but is significantly lower than the values (up to 15%) from other studies
6 [*Tuazon and Atkinson*, 1990; *Chuong and Stevens*, 2002; *Sprengnether et al.*, 2002]. The BASE
7 case rate constants for isoprene nitrate loss with OH and ozone are within the range estimated by
8 *Giacopelli et al.* [2005], but we find that the agreement with observations is only slightly
9 degraded using slower reaction rates (e.g., *Paulson and Seinfeld*, 1992; *Chen et al.*, 1998). We
10 find that the assumption of 40% NO_x recycling from ONITR+OH gives the best agreement with
11 observations, although a somewhat higher recycling rate could be supported, especially if the
12 production yield of isoprene nitrates were higher. The degree of recycling has not been well
13 constrained by previous studies, with *Paulson and Seinfeld* [1992] arguing that NO_x should be
14 released from this reaction, but other studies suggesting the formation of secondary
15 multifunctional nitrates [*Grossenbacher et al.*, 2001; *Giacopelli et al.*, 2005]. Finally, our results
16 suggest that isoprene nitrates are removed relatively quickly by dry deposition, as supported by
17 observations from *Rosen et al.* [2004] and *Horii et al.* [2006], but faster than suggested by
18 [*Shepson et al.*, 1996; *Giacopelli et al.*, 2005].

19
20 Most of the analysis in this paper has focused on the chemistry of the continental
21 boundary layer, where short-lived isoprene is abundant and isoprene nitrates are expected to
22 dominate ΣAN . In the boundary layer, we find that the BASE simulation best reproduces the
23 ICARTT observations of ΣAN concentrations and $\Delta\text{O}_3/\Delta\Sigma\text{AN}$ correlations. All of the

1 simulations presented here, however, considerably underestimate ΣAN in the free troposphere.
2 The speciated alkyl nitrates measured during ICARTT typically account for only ~10% of the
3 observed ΣANs even in the free troposphere, suggesting that the missing species are larger or
4 multifunctional nitrates. In the BASE simulation, which underestimates free tropospheric ΣAN
5 concentrations by a factor of 3, secondary multifunctional nitrates (XNITR) contribute over 90%
6 of the simulated total. The simulations that most closely match the free tropospheric observations
7 (4%_slowDD and 8%_slowDD; mean biases of -40% and -25%, respectively) overestimate ΣAN
8 by factors of 2-3 (and underestimate the $\Delta\text{O}_3/\Delta\Sigma\text{AN}$ correlation slope by a factor of 2 or more) in
9 the boundary layer. The simulations with 100% NO_x recycling (and no XNITR production) from
10 ONITR+OH (4%_100% NO_x and 8%_slowCHEM_100% NO_x) underestimate free tropospheric
11 concentrations by a factor of 15 or more. Based on the strong correlation between isoprene
12 nitrate export from the boundary layer (Figure 2) and free tropospheric ΣAN concentrations
13 (Figure 3) in our model, we estimate that a monthly export flux of ~50 GgN could enable the
14 model to reproduce observed free tropospheric ΣANs .

15
16 Possible causes of the underestimate of ΣANs in all simulations include insufficient
17 vertical mixing or other sources of organic nitrates in the free troposphere not represented in the
18 model. Insufficient vertical mixing out of the boundary layer could also account for the model
19 overestimate of NO_x and CO in Figure 1. While increased boundary layer ventilation would
20 decrease isoprene nitrate concentrations in the boundary layer, it would not be expected to alter
21 the simulated ratio $\Delta\text{O}_3/\Delta\Sigma\text{AN}$ dramatically, suggesting that constraints derived above from
22 boundary layer observations should be robust to a possible model bias in ventilation. High
23 isoprene nitrate export only occurs in our simulations, however, when boundary layer ΣAN

1 concentrations are strongly overestimated. In Figure 4, we evaluate the boundary layer
2 ventilation in the model by comparing simulated and observed vertical profiles of several
3 hydrocarbons with strong boundary layer sources (and their oxidation products). Based on the
4 lack of a systematic bias in the vertical gradients of these species, we find little evidence of
5 insufficient boundary layer ventilation in the model. Instead, the bias appears to be due to a
6 missing source of organic nitrates in the free troposphere. For instance, subsequent steps in the
7 oxidation of monoterpenes or other hydrocarbons, not adequately represented in our mechanism,
8 could lead to further production of organic nitrates. Also, our model treats both aldehydic and
9 hydroxy nitrates as a single species, whereas less efficient removal of the aldehydic nitrates by
10 wet and dry deposition could increase export and improve the simulation of free tropospheric
11 Σ ANs.

13 **4.3 Implications for NO_x budget**

14
15 We find that the formation of isoprene nitrates has a large effect on the NO_x budget in the
16 summertime boundary layer (Figure 2). In the BASE simulation, which best agrees with the
17 Σ AN and $\Delta\text{O}_3/\Delta\Sigma\text{AN}$ observations in the boundary layer (Figure 3), out of a total 519 GgN
18 surface NO_x emissions from the eastern United States in July, 79 GgN (15% of emissions) cycles
19 through isoprene nitrates. Once formed, 27 GgN (5% of emissions) is recycled from isoprene
20 nitrates back to NO_x within the continental boundary layer, 39 GgN (8% of emissions) are
21 removed permanently by dry and wet deposition, and 13 GgN (2% of emissions) are exported to
22 the free troposphere as isoprene nitrates. For comparison, *Horowitz et al.* [1998] estimated that
23 isoprene nitrate net chemical production (production minus loss from recycling) accounted for

1 16% of NO_x emissions the eastern United States in summer, with deposition and export of
2 isoprene nitrates equal to 14% and 1.5%, respectively. As discussed in Section 4.2, a much larger
3 export of ΣANs from the boundary layer (equal to $\sim 10\%$ of NO_x emissions) would be required to
4 match the free tropospheric observations of ΣANs (assuming no other free tropospheric source of
5 ΣANs).

6
7 We estimate a range for the values above by considering those simulations that agree best
8 with boundary layer observations of ΣANs and $\Delta\text{O}_3/\Delta\Sigma\text{AN}$ (Figure 3), excluding the simulations
9 with slow dry deposition and with 0% and 100% NO_x recycling. We thus estimate an
10 observationally constrained isoprene nitrate budget range of: production (79-96 GgN), recycling
11 to NO_x (23-33 GgN), deposition (39-51 GgN), and export (13-16 GgN). Note that this
12 constrained budget range is considerably narrower than the range that would be obtained if all
13 sensitivity simulations were considered, especially for the loss terms. The full range of losses is:
14 recycling to NO_x (0-73 GgN, 0-14% of NO_x emissions), deposition (10-57 GgN, 2-11%), and
15 export (2-41 GgN, 0.5-8%). The full range of isoprene nitrate production (76-100 GgN, 15-19%
16 of emissions) is similar to the constrained range above.

17
18 Isoprene nitrate chemistry affects ozone concentrations through its impact on the NO_x
19 budget. Uncertainties in the isoprene nitrate chemistry can alter the mean ozone mixing ratios in
20 the boundary layer by up to +3.0 ppbv (in simulation 4%_100 NO_x) and -2.0 ppbv (4%_0 NO_x)
21 from their BASE case values (Figure 1), demonstrating that recycling of NO_x from isoprene
22 nitrates can have a 5 ppbv impact on ozone. If we consider only the observationally constrained

1 simulations, the uncertainty range of mean ozone decreases to -1.4 to 0 ppbv from the BASE
2 case.

3 **5. Conclusions**

4
5 We combine model simulations and observations from the ICARTT field campaign over
6 the eastern United States during summer 2004 to constrain the chemistry of isoprene nitrates.
7 Simulated concentrations of trace species generally match observations to within 30% in the U.S.
8 boundary layer, except for NO_x (overestimated by ~30%) and PAN (overestimated by a factor of
9 ~2); free tropospheric concentrations of these species do not show this overestimate.
10 Comparisons of simulated tracer vertical profiles with observations suggest that the model
11 adequately represents boundary layer ventilation. Additional simulations are conducted to
12 examine the sensitivity of model results to assumptions about the following uncertain aspects of
13 isoprene chemistry: isoprene nitrate production yield, chemical loss rate, NO_x recycling, and dry
14 deposition. Observed concentrations of total hydroxyalkyl- and alkyl-nitrates (ΣANs) and the
15 correlation of ozone with ΣANs are used to constrain the possible values of the above
16 parameters. We find that our simulations with low deposition velocities for isoprene nitrates
17 produce unacceptably high boundary layer concentrations of ΣANs. Extreme rates of NO_x
18 recycling (0% or 100%) from the reaction of isoprene nitrates with OH lead to ΣAN
19 concentrations that are strongly biased (high or low, respectively) compared with observations,
20 but model results are relatively insensitive to the rate of this reaction. Finally, better agreement is
21 obtained with a lower isoprene nitrate production yield of 4% than with a higher yield of 8%.
22 The observations are best reproduced by the BASE and 4%_slowCHEM simulations, which

1 match the mean observed ΣAN concentrations in the boundary layer within 10-20%, and the
2 observed $\Delta\text{O}_3/\Delta\Sigma\text{AN}$ correlation slope (81.0 and 78.4 respectively in the model, 81.7 in the
3 observations).

4
5 Based on the evaluation of model results versus boundary layer observations, we find that
6 the most likely values for the parameters considered are: an isoprene nitrate yield from
7 ISOPO_2+NO of 4%, recycling of about half of ONITR to NO_x in the reactions with OH and
8 ozone, and fast removal of isoprene nitrates by dry deposition (at a rate similar to that of HNO_3).
9 We also identify a range of plausible values for these parameters based on other simulations
10 (4%_slowCHEM, 8%, 8%_slowCHEM). That is, slower loss of isoprene nitrates by reaction
11 with ozone and OH produces a negligible change in results, while an 8% yield of isoprene
12 nitrates slightly degrades agreement with observations, but cannot be ruled out. Of course, the set
13 of sensitivity experiments conducted here are not exhaustive of all possible values and
14 combinations of the parameters. For example, an 8% production yield of ONITR from
15 ISOPO_2+NO together with a somewhat higher rate of NO_x recycling might match observational
16 constraints as well as the BASE simulation. This possibility for cancellation of errors in our
17 model suggests the need for further laboratory and field studies of the chemistry and deposition
18 rates of isoprene nitrates.

19
20 We find that the NO_3 production pathway accounts for 49% of the total organic nitrate
21 production in the BASE case (with a range of ~40-50% in the observationally constrained
22 simulations, depending on the production yield of ONITR from ISOPO_2+NO), qualitatively
23 agreeing with the observational estimates of *Starn et al.* [1998]. The loss of isoprene nitrates

1 occurs primarily by dry deposition (~45%). Reactions with ozone and OH are responsible for
2 24% and 10%, respectively, of the isoprene nitrate loss in BASE. In simulations with slower
3 photochemical loss rates, these losses decrease to ~21% from ozone and ~8% from OH.
4

5 Isoprene nitrates are shown to have a major impact on the NO_x budget in the summertime
6 U.S. boundary layer. Based on constraints from boundary-layer observations, formation of
7 isoprene nitrates consumes 15-19% of the emitted NO_x (15% in the BASE simulation). Of this
8 amount, deposition of isoprene nitrates permanently removes 8-10% of NO_x emissions (8% in
9 BASE), 2-3% are exported (2% in BASE), and 4-6% are recycled to NO_x (5% in BASE). The
10 observed free tropospheric ΣAN concentrations could be matched by the model if the export of
11 nitrates were increased to ~10% of NO_x emissions. Through their impact on NO_x, isoprene
12 nitrates also affect surface ozone concentrations. The observational constraints serve to narrow
13 the uncertainty of this impact on ozone from 5.0 ppbv (varying from -2.0 to +3.0 ppbv from the
14 BASE case values) to 1.4 ppbv (-1.4 to 0 ppbv from BASE).
15

16 While we used available observations to constrain uncertainties in isoprene nitrate
17 chemistry, many uncertainties still exist and require further investigation. Our model budgets
18 indicate that the reaction of isoprene with NO₃ is the major pathway for isoprene nitrate
19 formation, but this pathway remains highly uncertain. The NO₃ pathway has not typically been
20 considered important for isoprene because of the diurnal anticorrelation between isoprene (which
21 peaks during mid-day) and NO₃ (which peaks at night). Since this pathway produces organic
22 nitrates with a much higher yield than the OH pathway (in our mechanism, ~80% yield versus 4-
23 8% for the OH pathway), however, it contributes significantly to isoprene nitrate production

1 even though it is only a minor pathway for isoprene loss (~6% in our model). In our model, the
2 rate of the isoprene+NO₃ reaction peaks in the hours after sunset, when NO₃ concentrations are
3 increasing and isoprene concentrations are decreasing following the cessation of emissions. The
4 degree of importance of this pathway for organic nitrate formation is sensitive, however, to the
5 details of the diurnal cycles of isoprene emissions and OH and NO₃ concentrations. We also find
6 that our model results are highly sensitive to the degree of recycling of NO_x from the reaction of
7 isoprene nitrates with OH. The amount of NO_x produced from this reaction, and the nature and
8 fate of the multifunctional organic nitrates formed, need further investigation. Finally, the large
9 discrepancy between simulated and observed ΣAN in the free troposphere suggests a
10 shortcoming in the representation of the chemistry of organic nitrates and/or their export in the
11 model. Based on the available measurements, it is not yet known whether these “missing”
12 nitrates are isoprene nitrates, or nitrates derived from other parent hydrocarbons.

13 **References**

- 14
- 15 Aschmann, S.M., R. Atkinson, and J. Arey (2002), Products of reaction of OH radicals with α-
16 pinene, *J. Geophys. Res.*, *107*(D14), 4191, doi:10.1029/2001JD001098.
- 17
- 18 Bey, I., D.J. Jacob, R.M. Yantosca, J.A. Logan, B.D. Field, A.M. Fiore, Q. Li, H.Y. Liu, L.J.
19 Mickley, and M.G. Schultz (2001), Global modeling of tropospheric chemistry with
20 assimilated meteorology: Model description and evaluation, *J. Geophys. Res.*, *106*,
21 23,073-23,095.
- 22

1 Blake, N.J., and 16 others (2003), NMHCs and halocarbons in Asian continental outflow during
2 the Transport and Chemical Evolution over the Pacific (TRACE-P) Field Campaign:
3 Comparison With PEM-West B, *J. Geophys. Res.*, *108*(D20), 8806,
4 doi:10.1029/2002JD003367.

5

6 Chen, X., D. Hulbert, and P.B. Shepson (1998), Measurement of the organic nitrate yield from
7 OH reaction with isoprene, *J. Geophys. Res.*, *103*(D19), 25,563-25,568.

8

9 Chuong B., and P. S. Stevens (2002), Measurements of the kinetics of the OH-initiated oxidation
10 of isoprene, *J. Geophys. Res.*, *107*(D13), 4162, doi:10.1029/2001JD000865.

11

12 Cleary, P.A., J.G. Murphy, P.J. Wooldridge, D.A. Day, D.B. Millet, M. McKay, A.H. Goldstein,
13 and R.C. Cohen (2005), Observations of total alkyl nitrates within the Sacramento Urban
14 Plume, *Atmos. Chem. Phys. Discuss.*, *5*, 4801-4843.

15

16 Crounse, J., P. Wennberg, A. Kwan, B. Heikes, D. O'Sullivan, H. Shen, and J. Crawford (2006),
17 Peroxyacetic acid is ubiquitous in the upper troposphere, submitted to *Geophys. Res.*
18 *Lett.*.

19

20 Day, D.A., P.J. Wooldridge, M. Dillon, J.A. Thornton, and R.C. Cohen (2002), A thermal
21 dissociation-laser induced fluorescence instrument for in-situ detection of NO₂,
22 peroxy(acyl)nitrates, alkyl nitrates, and HNO₃., *J. Geophys. Res.*, *107*(D6),
23 10.1029/2001JD000779.

- Day, D.A., M.B. Dillon, P.J. Wooldridge, J.A. Thornton, R.S. Rosen, E.C. Wood, and R.C. Cohen (2003), On Alkyl Nitrates, Ozone and the 'Missing NO_y', *J. Geophys. Res.*, *108*(D16), 10.1029/2003JD003685.
- de Gouw, J.A., P.D. Goldan, C. Warneke, W.C. Kuster, J.M. Roberts, M. Marchewka, S.B. Bertman, A.A.P. Pszenny, and W.C. Keene (2003), Validation of proton transfer reaction-mass spectrometry (PTR-MS) measurements of gas-phase organic compounds in the atmosphere during the New England Air Quality Study (NEAQS) in 2002, *J. Geophys. Res.*, *108*(D21), 4682, doi:10.1029/2003JD003863.
- de Gouw, J.A., C. Warneke, A. Stohl, A.G. Wollny, C.A. Brock, O.R. Cooper, J.S. Holloway, M. Trainer, F.C. Fehsenfeld, E.L. Atlas, S.G. Donnelly, V. Stroud, and A. Lueb (2006), The VOC composition of aged forest fire plumes from Alaska and western Canada, *J. Geophys. Res.*, *111*, D10303, doi:10.1029/2005JD006175.
- Fan, J., and R. Zhang, Atmospheric oxidation mechanism of isoprene (2004), *Environ. Chem.*, *1*, 140-149, doi:10.1071/EN04045.
- Fehsenfeld, F.C., et al. (2006), International Consortium for Atmospheric Research on Transport and Transformation (ICARTT): North America to Europe—Overview of the 2004 summer field study, *J. Geophys. Res.*, *111*, D23S01, doi:10.1029/2006JD007829.

1 Fiore, A. M., L. W. Horowitz, D. W. Purves, H. Levy II, M. J. Evans, Y. Wang, Q. Li, and R. M.
 2 Yantosca (2005), Evaluating the contribution of changes in isoprene emissions to surface
 3 ozone trends over the eastern United States, *J. Geophys. Res.*, *110*, D12303,
 4 doi:10.1029/2004JD005485.
 5
 6 Fried, A., J. Walega, J. Olson, J. Crawford, G. Chen, B. Heikes, D. O'Sullivan, H. Shen, et al.
 7 (2006), The role of convection in redistributing formaldehyde to the upper troposphere
 8 over North America and the North Atlantic during the Summer 2004 INTEX campaign,
 9 submitted to *J. Geophys. Res.*.
 10
 11 Frost, G. J., S.A. McKeen, M. Trainer, T.B. Ryerson, J.A. Neuman, J.M. Roberts, A. Swanson,
 12 J.S. Holloway, D.T. Sueper, T. Fortin, D.D. Parrish, F.C. Fehsenfeld, F. Flocke, S.E.
 13 Pechkam, G.A. Grell, D. Kowal, J. Cartwright, N. Auerbach, and T. Habermann (2006),
 14 Effects of changing power plant NO_x emissions on ozone in the eastern United States:
 15 Proof of concept, *J. Geophys. Res.*, *111*, D12306, doi:10.1029/2005JD006354.
 16
 17 Giacomelli, P., K. Ford, C. Espada, and P.B. Shepson (2005), Comparison of the measured and
 18 simulated isoprene nitrate distributions above a forest canopy, *J. Geophys. Res.*, *110*,
 19 D01304, doi:10.1029/2004JD005123.
 20
 21 Grossenbacher, J.W., T. Couch, P.B. Shepson, T. Thornberry, M. Witmer-Rich, M.A. Carroll, I.
 22 Faloona, D. Tan, W. Brune, K. Ostling, and S. Bertman (2001), Measurements of
 23 isoprene nitrates above a forest canopy, *J. Geophys. Res.*, *106*(D20), 24,429-24,438.

Grossenbacher, J.W., D.J. Barket Jr., P.B. Shepson, M.A. Carroll, K. Olszyna, and E. Apel
(2004), A comparison of isoprene nitrate concentrations at two forest-impacted sites, *J. Geophys. Res.*, *109*, D11311, doi: 10.1029/2003JD003966.

Guenther, A., C.N. Hewitt, D. Erickson, R. Fall, C. Geron, T. Graedel, P. Harley, L. Klinger, M. Lerdau, W.A. McKay, T. Pierce, B. Scholes, R. Steinbrecher, R. Tallamraju, J. Taylor, and P. Zimmerman (1995), A global model of natural volatile organic carbon emissions, *J. Geophys. Res.*, *100*, 8873-8892.

Guenther, A., T. Karl, P. Harley, C. Wiedinmyer, P. I. Palmer, and C. Geron (2006), Estimates of global terrestrial isoprene emissions using MEGAN (Model of Emissions of Gases and Aerosols from Nature), *Atmos. Chem. Phys.*, *6*, 3181-3210.

Holloway, J.S., R.O. Jakoubek, D.D. Parrish, C. Gerbig, A. Volz-Thomas, S. Schmitgen, A. Fried, B. Wert, B. Henry, and J.R. Drummond (2000), Airborne intercomparison of vacuum ultraviolet fluorescence and tunable diode laser absorption measurements of tropospheric carbon monoxide, *J. Geophys. Res.*, *105*, 24,251-24,262.

Horii, C.V., J.W. Munger, S.C. Wofsy, M. Zahniser, D. Nelson, and J.B. McManus (2006), Atmospheric reactive nitrogen concentration and flux budgets at a Northeastern U.S. forest site, *Ag. For. Met.*, *136*, 159-174.

- 1 Horowitz, L.W., J. Liang, G.M. Gardner, and D.J. Jacob (1998), Export of reactive nitrogen from
2 North America during summertime: Sensitivity to hydrocarbon chemistry, *J. Geophys.*
3 *Res.*, *103*, 13,451– 13,476.
- 4
- 5 Horowitz, L.W., S. Walters, D.L. Mauzerall, L.K. Emmons, P.J. Rasch, C. Granier, X.X. Tie, J.-
6 F. Lamarque, M.G. Schultz, G.S. Tyndall, J.J. Orlando, and G.P. Brasseur (2003), A
7 global simulation of tropospheric ozone and related tracers: Description and evaluation of
8 MOZART, version 2, *J. Geophys. Res.*, *108*(D24), 4784, doi:10.1029/2002JD002853.
- 9
- 10 Houweling, S., F. Dentener, and J. Lelieveld (1998), The impact of non-methane hydrocarbon
11 compounds on tropospheric photochemistry, *J. Geophys. Res.*, *103*, 10,673-10,696.
- 12
- 13 Kwok, E.S.C., and R. Atkinson (2005), Estimation of hydroxyl radical reaction rate constants for
14 gas-phase organic compounds using a structure-reactivity relationship: An update, *Atmos.*
15 *Environ.*, *29*, 1685-1695.
- 16
- 17 Madronich, S., and S. Flocke (1998), The role of solar radiation in atmospheric chemistry, in
18 *Handbook of Environmental Chemistry*, edited by P. Boule, pp. 1-26, Springer-Verlag,
19 New York.
- 20
- 21 Neeb, P. (2000), Structure-reactivity based estimation of the rate constants for hydroxyl radical
22 reactions with hydrocarbons, *J. Atmos. Chem.*, *35*, 295-315.
- 23

Nozière, B., I. Barnes, and K. Becker (1999), Product study and mechanisms of the reactions of α -pinene and of pinonaldehyde with OH radicals, *J. Geophys. Res.*, *104*(D19), 23,645-23,656.

O'Brien, J.M., P.B. Shepson, K. Muthuramu, C. Hau, H. Niki, D.R. Hastie, R. Taylor, and P.B. Roussel (1995), Measurement of alkyl and multifunctional organic nitrates at a rural site in Ontario, *J. Geophys. Res.*, *100*, 22,795-22,804.

Paulson, S.E. and J.H. Seinfeld (1992), Development and evaluation of a photooxidation mechanism for isoprene, *J. Geophys. Res.*, *97*, 20,703-20,715.

Pierce, T., C. Geron, L. Bender, R. Dennis, G. Tonnesen, and A. Guenther (1998), Influence of increased isoprene emissions on regional ozone modeling, *J. Geophys. Res.*, *103*, 25,611-25,629.

Pöschl, U., R. von Kuhlmann, N. Poisson, and P.J. Crutzen (2000), Development and intercomparison of condensed isoprene oxidation mechanisms for global atmospheric modeling, *J. Atmos. Chem.*, *37*, 29-52.

Purves, D.W., J.P. Caspersen, P.R. Moorcroft, G.C. Hurtt, and S.W. Pacala (2004), Human-induced changes in U.S. biogenic VOC emissions: Evidence from long-term forest inventory data, *Global Change Biol.*, *10*, 1-19, doi:10.1111/j.1365-2486.2004.00844.x.

1 Ren, X., Brune, W.H., J. Mao, R.B. Long, R.L. Lesher, J.H. Crawford, J.R. Olson, G. Chen,
 2 M.A. Avery, G.W. Sachse, G.S. Diskin, J.D. Barrick, L.G. Huey, A. Fried, R.C. Cohen,
 3 B. Heike, P. Wennberg, H.B. Singh, D.R. Blake, and R.E. Shetter (2006), HO_x
 4 observation and model comparison during INTEX-NA 2004, submitted to *J. Geophys.*
 5 *Res.*.
 6
 7 Roller, C., A. Fried, J. Walega, P. Weibring, and F. Tittel (2006), Advances in hardware, system
 8 diagnostics software, and acquisition procedures for high performance airborne tunable
 9 diode laser measurements of formaldehyde, *Appl. Phys. B*, 82, 247-264,
 10 doi:10.1007/s00340-005-1998-8.
 11
 12 Rosen, R.S., E.C. Wood, P.J. Wooldridge, J.A. Thornton, D.A. Day, W. Kuster, E.J. Williams,
 13 B.T. Jobson, and R.C. Cohen (2004), Observations of total alkyl nitrates during Texas
 14 Air Quality Study 2000: Implications for O₃ and alkyl nitrate photochemistry, *J.*
 15 *Geophys. Res.*, 109(D7), D07303, doi:10.1029/2003JD004227.
 16
 17 Ryerson, T.B., and 30 others (2003), Effect of petrochemical industrial emissions of reactive
 18 alkenes and NO_x on tropospheric ozone formation in Houston, Texas, *J. Geophys. Res.*,
 19 108(D8), 4249, doi:10.1029/2002JD003070.
 20
 21 Sachse, G. W., G.F. Hill, L.O. Wade, and M.G. Perry (1987), Fast-response, high-precision
 22 carbon monoxide sensor using a tunable diode laser absorption technique, *J. Geophys.*
 23 *Res.*, 92, 2071-2081.

- 1
2 Shepson, P.B., E. Mackay, and K. Muthuramu (1996), Henry's law constants and removal
3 processes for several atmospheric β -hydroxy alkyl nitrates, *Environ. Sci. Technol.*, 30,
4 3618-3623.
5
- 6 Shim, C., Wang, Y., Choi, Y., Palmer, P., Abbot, D., and Chance, K. (2005), Constraining global
7 isoprene emissions with Global Ozone Monitoring Experiment (GOME) formaldehyde
8 column measurements, *J. Geophys. Res.*, 110(D24), D24301,
9 doi:10.1029/2004JD005629.
10
- 11 Sillman, S., and P. J. Samson (1995), Impact of temperature on oxidant photochemistry in urban,
12 polluted rural and remote environments, *J. Geophys. Res.*, 100(D6), 11,497-11,508,
13 10.1029/94JD02146.
14
- 15 Singh, H., Y. Chen, A. Tabazadeh, Y. Fukui, I. Bey, R. Yantosca, D. Jacob, F. Arnold,
16 K. Wohlfarth, E. Atlas, F. Flocke, D. Blake, N. Blake, B. Heikes, J. Snow, R. Talbot,
17 G. Gregory, G. Sachse, S. Vay, and Y. Kondo (2000), Distribution and fate of selected
18 oxygenated organic species in the troposphere and lower stratosphere over the Atlantic, *J.*
19 *Geophys. Res.*, 105(D3), 3795-3806.
20
- 21 Singh H.B., W.H. Brune, J.H. Crawford, D.J. Jacob, and P.B. Russell (2006), Overview of the
22 Summer 2004 Intercontinental Chemical Transport Experiment-North America (INTEX-
23 A), *J. Geophys. Res.*, 111, D24S01, doi:10.1029/2006JD007905.
24

1 Singh, H.B., L. Salas, D. Herlth, R. Kolyer, E. Czech, M. Avery, J.H. Crawford, G.W. Sachse,
2 D.R. Blake, R.C. Cohen, J. Dibb, G. Huey, R.C. Hudman, D.J. Jacob, L.K. Emmons,
3 L.W. Horowitz, F. Flocke, Y. Tang, and G.R. Carmichael (2007), Reactive nitrogen
4 distribution and partitioning in the North American troposphere and lowermost
5 stratosphere, submitted to *J. Geophys. Res.*.

6
7 Slusher, D. L., L. G. Huey, D. J. Tanner, F. M. Flocke, and J. M. Roberts (2004), A thermal
8 dissociation-chemical ionization mass spectrometry (TD-CIMS) technique for the
9 simultaneous measurement of peroxyacyl nitrates and dinitrogen pentoxide, *J. Geophys.*
10 *Res.*, *109*, D19315, doi:10.1029/2004JD004670.

11
12 Sprengnether, M., K.L. Demerjian, N.M. Donahue, and J.G. Anderson (2002), Product analysis
13 of the OH oxidation of isoprene and 1,3-butadiene in the presence of NO, *J. Geophys.*
14 *Res.*, *107*(D15), doi:10.1029/2001JD000716.

15
16 Starn, T.K., P.B. Shepson, S.B. Bertman, D.D. Riemer, R.G. Zika, and K. Olszyna (1998),
17 Nighttime isoprene chemistry at an urban-impacted forest site, *J. Geophys. Res.*,
18 *103*(D17), 22,437-22,448.

19
20 Thornton, J.A., P.J. Wooldridge, and R.C. Cohen (2000), Atmospheric NO₂: In situ laser-induced
21 fluorescence detection at parts per trillion mixing ratios, *Anal. Chem.*, *72*, 528-539,
22 doi:10.1021/ac9908905.

Trainer, M., E.J. Williams, D.D. Parrish, M.P. Buhr, E.J. Allwine, H.H. Westberg, F.C. Fehsenfeld, and S.C. Liu (1987), Models and observations of the impact of natural hydrocarbons on rural ozone, *Nature*, 329, 705-707.

Trainer, M., M.P. Buhr, C.M. Curran, F.C. Fehsenfeld, E.Y. Hsie, S.C. Liu, R.B. Norton, D.D. Parrish, E.J. Williams, B.W. Gandrud, B.A. Ridley, J.D. Shetter, E.J. Allwine, and H.H. Westberg (1991), Observations and modeling of the reactive nitrogen photochemistry at a rural site, *J. Geophys. Res.*, 96(D2), 3045-3063.

Treves, K., and Y. Rudich, The atmospheric fate of C₃-C₆ hydroxyalkyl nitrates (2003), *J. Phys. Chem. A*, 107, 7809-7817.

Turnipseed, A.A., L.G. Huey, E. Nemitz, R. Stickel, J. Higgs, D.J. Tanner, D.L. Slusher, J.P. Sparks, F. Flocke, and A. Guenther (2006), Eddy covariance fluxes of peroxyacetyl nitrates (PANs) and NO_y to a coniferous forest, *J. Geophys. Res.*, 111, D09304, doi:10.1029/2005JD006631.

Turquety, S., J.A. Logan, D.J. Jacob, R.C. Hudman, F.Y. Leung, C.L. Heald, R.M. Yantosca, S. Wu, L.K. Emmons, D.P. Edwards, and G.W. Sachse (2007), Inventory of boreal fire emissions for North America in 2004: The importance of peat burning and pyro-convective injection, *J. Geophys. Res.*, in press.

1 Vay, S.A., B.E. Anderson, G.W. Sachse, J.E. Collins Jr., J.R. Podolske, C.H. Twohy, B.
2 Gandrud, K.R. Chan, S.L. Baughcum, and H.A. Wallio (1998), DC-8-based observations
3 of aircraft CO, CH₄, N₂O, and H₂O(g) emission indices during SUCCESS, *Geophys. Res.*
4 *Lett.*, 25, 1717-1720.

5

6 von Kuhlmann, R., M.G. Lawrence, U. Pöschl, and P.J. Crutzen (2004), Sensitivities in global
7 scale modeling of isoprene, *Atmos. Chem. Phys.*, 4, 1-17.

8

9 Wu, S., L.J. Mickley, D.J. Jacob, J.A. Logan, R.M. Yantosca, and D. Rind (2007), Why are there
10 large differences between models in global budgets of tropospheric ozone?, *J. Geophys.*
11 *Res.*, in press.

- 1 **Table 1.** Isoprene and monoterpene mechanism used in base model simulations. Second-order
- 2 reaction rate constants are given in units of $\text{molec}^{-1} \text{cm}^3 \text{s}^{-1}$.

Reaction	Rate Constant
$\text{ISOP} + \text{OH} \rightarrow \text{ISOP} \text{O}_2$	$2.54\text{E-}11 \cdot \exp(410/T)$
$\text{ISOP} + \text{O}_3 \rightarrow .4 \cdot \text{MACR} + .2 \cdot \text{MVK} + .07 \cdot \text{C}_3\text{H}_6 + .27 \cdot \text{OH} + .06 \cdot \text{HO}_2 + .6 \cdot \text{CH}_2\text{O} + .3 \cdot \text{CO} + .1 \cdot \text{O}_3 + .2 \cdot \text{MCO}_3 + .2 \cdot \text{CH}_3\text{COOH}$	$1.05\text{E-}14 \cdot \exp(-2000/T)$
$\text{ISOP} + \text{NO}_3 \rightarrow \text{ISOPNO}_3$	$3.03\text{E-}12 \cdot \exp(-446/T)$
$\text{ISOP} \text{O}_2 + \text{NO} \rightarrow .04 \cdot \text{ONITR} + .96 \cdot \text{NO}_2 + \text{HO}_2 + .57 \cdot \text{CH}_2\text{O} + .24 \cdot \text{MACR} + .33 \cdot \text{MVK} + .38 \cdot \text{HYDRALD}$	$2.20\text{E-}12 \cdot \exp(180/T)$
$\text{ISOP} \text{O}_2 + \text{NO}_3 \rightarrow \text{HO}_2 + \text{NO}_2 + .6 \cdot \text{CH}_2\text{O} + .25 \cdot \text{MACR} + .35 \cdot \text{MVK} + .4 \cdot \text{HYDRALD}$	$2.40\text{E-}12$
$\text{ISOP} \text{O}_2 + \text{HO}_2 \rightarrow \text{ISOP} \text{OOH}$	$8.00\text{E-}13 \cdot \exp(700/T)$
$\text{ISOP} \text{O}_2 + \text{CH}_3\text{O}_2 \rightarrow .25 \cdot \text{CH}_3\text{OH} + \text{HO}_2 + 1.2 \cdot \text{CH}_2\text{O} + .19 \cdot \text{MACR} + .26 \cdot \text{MVK} + .3 \cdot \text{HYDRALD}$	$5.00\text{E-}13 \cdot \exp(400/T)$
$\text{ISOP} \text{O}_2 + \text{CH}_3\text{CO}_3 \rightarrow \text{CH}_3\text{O}_2 + \text{HO}_2 + .6 \cdot \text{CH}_2\text{O} + .25 \cdot \text{MACR} + .35 \cdot \text{MVK} + .4 \cdot \text{HYDRALD}$	$1.40\text{E-}11$
$\text{MVK} + h\nu \rightarrow .7 \cdot \text{C}_3\text{H}_6 + .7 \cdot \text{CO} + .3 \cdot \text{CH}_3\text{O}_2 + .3 \cdot \text{CH}_3\text{CO}_3$	Photolysis
$\text{MVK} + \text{OH} \rightarrow \text{MACR} \text{O}_2$	$4.13\text{E-}12 \cdot \exp(452/T)$
$\text{MVK} + \text{O}_3 \rightarrow .8 \cdot \text{CH}_2\text{O} + .95 \cdot \text{CH}_3\text{COCHO} + .08 \cdot \text{OH} + .2 \cdot \text{O}_3 + .06 \cdot \text{HO}_2 + .05 \cdot \text{CO} + .04 \cdot \text{CH}_3\text{CHO}$	$7.52\text{E-}16 \cdot \exp(-1521/T)$
$\text{MACR} + h\nu \rightarrow .67 \cdot \text{HO}_2 + .33 \cdot \text{MCO}_3 + .67 \cdot \text{CH}_2\text{O} + .67 \cdot \text{CH}_3\text{CO}_3 + .33 \cdot \text{OH} + .67 \cdot \text{CO}$	Photolysis
$\text{MACR} + \text{OH} \rightarrow .5 \cdot \text{MACR} \text{O}_2 + .5 \cdot \text{H}_2\text{O} + .5 \cdot \text{MCO}_3$	$1.86\text{E-}11 \cdot \exp(175/T)$
$\text{MACR} + \text{O}_3 \rightarrow .8 \cdot \text{CH}_3\text{COCHO} + .275 \cdot \text{HO}_2 + .2 \cdot \text{CO} + .2 \cdot \text{O}_3 + .7 \cdot \text{CH}_2\text{O} + .215 \cdot \text{OH}$	$4.40\text{E-}15 \cdot \exp(-2500/T)$

Reaction	Rate Constant
MACRO2 + NO \rightarrow NO2 + .47*HO2 + .25*CH2O + .25*CH3COCHO + .53*CH3CO3 + .53*GLYALD + .22*HYAC + .22*CO	2.70E-12*exp(360/T)
MACRO2 + NO \rightarrow ONITR	1.30E-13*exp(360/T)
MACRO2 + NO3 \rightarrow NO2 + .47*HO2 + .25*CH2O + .25*CH3COCHO + .22*CO + .53*GLYALD + .22*HYAC + .53*CH3CO3	2.40E-12
MACRO2 + HO2 \rightarrow MACROOH	8.00E-13*exp(700/T)
MACRO2 + CH3O2 \rightarrow .73*HO2 + .88*CH2O + .11*CO + .24*CH3COCHO + .26*GLYALD + .26*CH3CO3 + .25*CH3OH + .23*HYAC	5.00E-13*exp(400/T)
MACRO2 + CH3CO3 \rightarrow .25*CH3COCHO + CH3O2 + .22*CO + .47*HO2 + .53*GLYALD + .22*HYAC + .25*CH2O + .53*CH3CO3	1.40E-11
ISOPOOH + hv \rightarrow .402*MVK + .288*MACR + .69*CH2O + HO2	Photolysis
ISOPOOH + OH \rightarrow .5*XO2 + .5*ISOPO2	3.80E-12*exp(200/T)
MACROOH + OH \rightarrow .5*MCO3 + .2*MACRO2 + .1*OH + .2*HO2	2.30E-11*exp(200/T)
ONITR + hv \rightarrow HO2 + CO + NO2 + CH2O	Photolysis
ONITR + OH \rightarrow .4*HYDRALD + .4*NO2 + HO2 + .6*XNITR	4.50E-11
ONITR + O3 \rightarrow .4*HYDRALD + .4*NO2 + HO2 + .6*XNITR	1.30E-16
ONITR + NO3 \rightarrow NO2 + HO2 + XNITR	1.40E-12*exp(-1860/T)
ISOPNO3 + NO \rightarrow 1.206*NO2 + .794*HO2 + .072*CH2O + .167*MACR + .039*MVK + .794*ONITR	2.70E-12*exp(360/T)
ISOPNO3 + NO3 \rightarrow 1.206*NO2 + .072*CH2O + .167*MACR + .039*MVK + .794*ONITR + .794*HO2	2.40E-12

Reaction	Rate Constant
ISOPNO3 + HO2 → .206*NO2 + .794*HO2 + .008*CH2O + .167*MACR + .039*MVK + .794*ONITR	8.00E-13*exp(700/T)
C10H16 + OH → TERPO2	1.20E-11*exp(444/T)
C10H16 + O3 → .7*OH + MVK + MACR + HO2	1.00E-15*exp(-732/T)
C10H16 + NO3 → TERPO2 + NO2	1.20E-12*exp(490/T)
TERPO2 + NO → .1*CH3COCH3 + HO2 + .82*MVK + .82*MACR + .82*NO2 + .18*ONITR	4.20E-12*exp(180/T)
TERPO2 + HO2 → TERPOOH	7.50E-13*exp(700/T)
TERPOOH + hv → OH + .1*CH3COCH3 + HO2 + MVK + MACR	Photolysis
TERPOOH + OH → TERPO2	3.80E-12*exp(200/T)

1 **Table 2.** Sensitivity simulations in MOZART-4 model.

Simulation	Yield ¹	Loss rate ²	Deposition ³	NO _x recycling ⁴	Isoprene nitrate burden ⁵ (GgN)	Isoprene nitrate lifetime ⁶ (hrs)
4% (BASE)	4%	Fast	Fast	40%	1.46	13.8
4%_slowCHEM	4%	Slow	Fast	40%	1.53	14.5
4%_slowDD	4%	Fast	Slow	40%	3.03	28.5
8%	8%	Fast	Fast	40%	1.82	14.0
8%_slowCHEM	8%	Slow	Fast	40%	1.91	14.8
8%_slowDD	8%	Fast	Slow	40%	3.76	28.9
4%_0%NOx	4%	Fast	Fast	0%	2.27	22.2
4%_100%NOx	4%	Fast	Fast	100%	0.13	1.1
8%_slowCHEM_100%NOx	8%	Slow	Fast	100%	0.36	2.7

2 ¹Yield of isoprene nitrates (ONITR) from the reaction of isoprene peroxy radicals (ISOPO2) with NO.

3 ²Loss rates of ONITR. “Fast” indicates $k(\text{ONITR}+\text{OH}) = 4.5 \times 10^{-11} \text{ molec}^{-1} \text{ cm}^3 \text{ s}^{-1}$, $k(\text{ONITR}+\text{O}_3) = 1.30 \times 10^{-16}$, $J(\text{ONITR}) =$

4 $J(\text{CH}_3\text{CHO})$. “Slow” indicates $k(\text{ONITR}+\text{OH}) = 1.3 \times 10^{-11}$, $k(\text{ONITR}+\text{O}_3) = 4.33 \times 10^{-17}$, $J(\text{ONITR}) = J(\text{HNO}_3)$.

5 ³Rate of ONITR (and XNITR) dry deposition. “Fast” indicates $V_d(\text{ONITR}) = V_d(\text{HNO}_3)$. “Slow” indicates $V_d(\text{ONITR}) = V_d(\text{PAN})$. In

6 both cases, wet deposition is based on a Henry’s Law constant of $H_{298}(\text{ONITR}) = 7.51 \times 10^3 \text{ M atm}^{-1}$.

- 1 ⁴Recycling of NO_x from reactions of ONITR with OH and ozone. The balance of the reactive nitrogen produces multifunctional
2 organic nitrates (XNITR).
- 3 ⁵Mean burden of isoprene nitrates (ONITR+XNITR+ISOPNO₃) in the eastern United States (24-52°N, 62.5-97.5°W) boundary layer
4 (below 800 hPa) during July 2004.
- 5 ⁶Mean lifetime of isoprene nitrates (ONITR+XNITR+ISOPNO₃) in the eastern United States boundary layer during July 2004 versus
6 all loss processes shown in Figure 2.

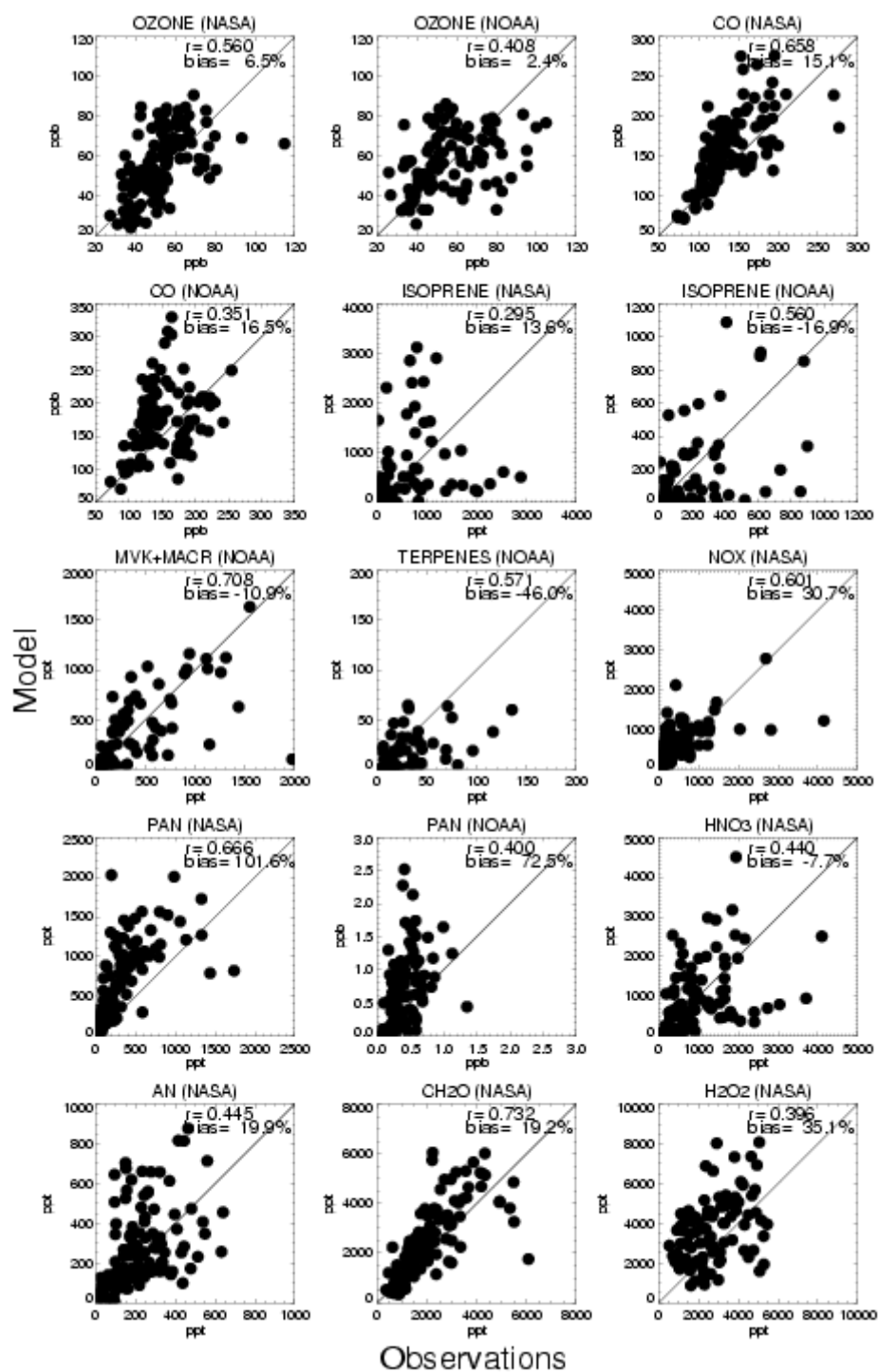
Figure Captions

Figure 1. MOZART-4 model versus observed concentrations of selected trace species for daytime observations (1500-2300 UTC) below 2 km in the eastern United States (24-52°N, 62.5-97.5°W). Hourly model results are sampled at the locations of 1-minute observations. The 1-minute model values and observations for each NOAA WP-3D and NASA DC-8 flight are then averaged onto the model grid. Observations shown from the NASA DC-8 are: ozone (PI: Avery, chemiluminescence), CO (PI: Sachse differential absorption TDL spectrometer) [Sachse *et al.*, 1987; Vay *et al.*, 1998]), isoprene (PI: D. Blake, whole-air sample, gas chromatography) [Blake *et al.*, 2003], NO_x = NO (PI: Brune) [Ren *et al.*, 2006] + NO₂ (PI: Cohen, laser induced fluorescence) [Thornton *et al.*, 2000], PAN (PI: Singh, electron-capture gas chromatography) [Singh *et al.*, 2000, 2007], HNO₃ and H₂O₂ (PI: Wennberg, chemical ionization mass spectrometer) [Crounse *et al.*, 2006], total alkyl- and hydroxyalkyl-nitrates (AN, PI: Cohen, thermal dissociation - laser induced fluorescence) [Day *et al.*, 2002; Cleary *et al.*, 2005] and CH₂O (PI: Fried, TDLAS) [Roller *et al.*, 2006, and references therein; Fried *et al.*, 2006]. Observations shown from the NOAA WP-3D are: ozone (PI: Ryerson, chemiluminescence) [Ryerson *et al.*, 2003], CO (PI: Holloway, vacuum UV fluorescence) [Holloway *et al.*, 2000], isoprene, methylvinyl ketone + methacrolein (MVK+MACR), and monoterpenes (PIs: de Gouw and Warneke, PTR-MS) [de Gouw *et al.*, 2003, 2006], and PAN (PI: Flocke, thermal dissociation-chemical ionization mass spectrometry) [Slusher *et al.*, 2004].

Figure 2. Budgets of isoprene nitrates (ONITR+XNITR+ISOPNO₃) in the eastern United States (24-52°N, 62.5-97.5°W) boundary layer (below 800 hPa) during July 2004 for each model simulation. Production of isoprene nitrates occurs from terpenes (pinene), methylvinyl ketone and methacrolein (MACR), and from isoprene reactions with NO₃ (NO₃) and OH (ISOP). Loss occurs via photolysis and vertical diffusion (hv+DIF), reaction with OH (OH), wet deposition (WD), advection (ADV), convection (CNV), and dry deposition (DD).

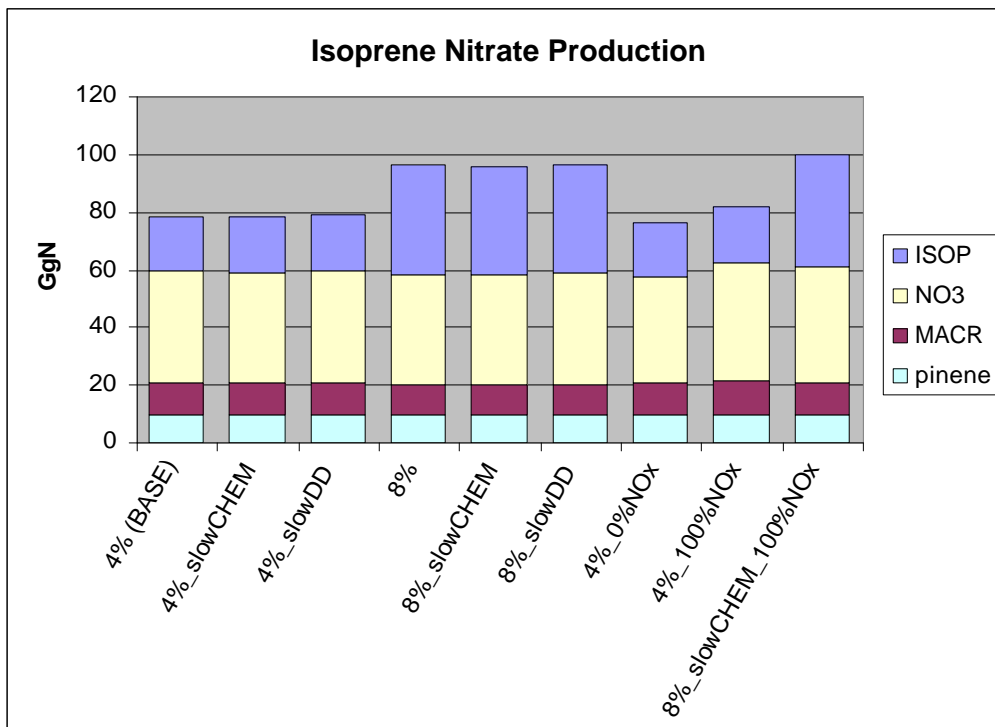
Figure 3. Mean ICARTT vertical profile of the sum of all alkyl nitrates (Σ AN) from observations (black, standard deviations indicated by horizontal bars) and model (colored by simulation as shown in legend; see also Table 2) from all DC-8 flights (left). Correlation plot of ozone versus Σ AN and reduced major axis regression line from observations (black points and line) and model (colored points and lines) for daytime (1500-2300 UTC) DC-8 data over the eastern United States (24-52°N, 62.5-97.5°W) (right). Hourly model results are sampled at the locations of the 1-minute observations. In the ozone- Σ AN correlation plot, 1-minute data points for each flight have been averaged onto the model grid.

Figure 4. Mean ICARTT vertical profiles of CO, isoprene, methylvinyl ketone + methacrolein, ethane, and propane from observations on the NASA DC-8 and NOAA WP-3D (black, standard deviations indicated by horizontal bars) and model sampled along the appropriate flight tracks (red). Hourly model results are sampled at the locations of the 1-minute observations.

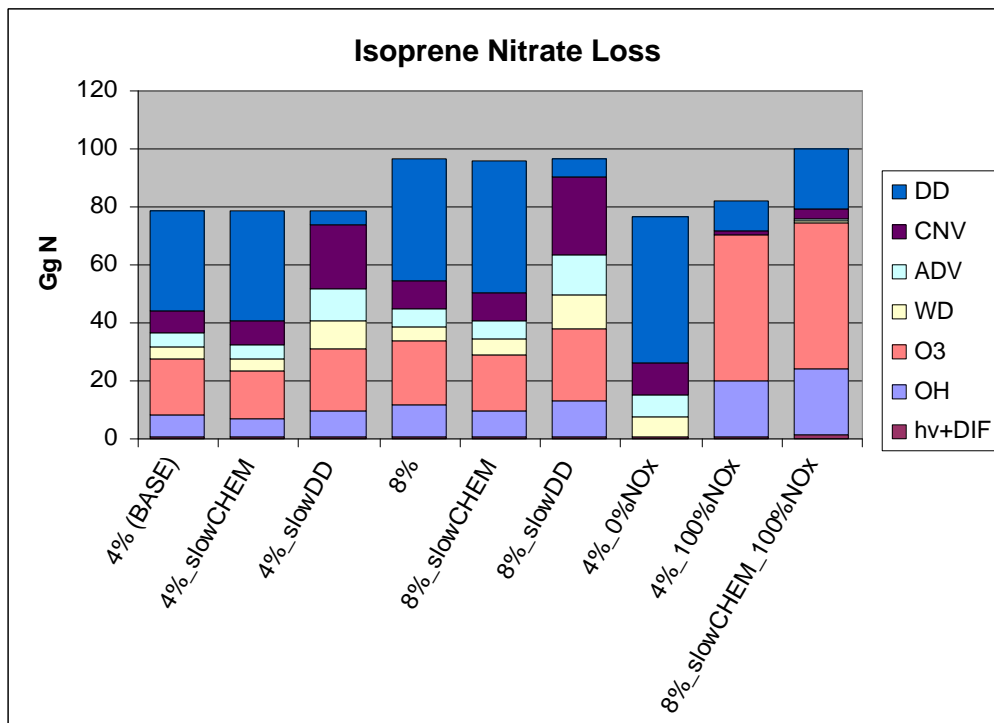


1
2 **Figure 1.** MOZART-4 model versus observed concentrations of selected trace species for
3 daytime observations (1500-2300 UTC) below 2 km in the eastern United States (24-52°N, 62.5-
4 97.5°W). Hourly model results are sampled at the locations of 1-minute observations. The 1-

1 minute model values and observations for each NOAA WP-3D and NASA DC-8 flight are then
2 averaged onto the model grid. Observations shown from the NASA DC-8 are: ozone (PI: Avery,
3 chemiluminescence), CO (PI: Sachse differential absorption TDL spectrometer) [*Sachse et al.*,
4 1987; *Vay et al.*, 1998]), isoprene (PI: D. Blake, whole-air sample, gas chromatography) [*Blake*
5 *et al.*, 2003], $\text{NO}_x = \text{NO}$ (PI: Brune) [*Ren et al.*, 2006] + NO_2 (PI: Cohen, laser induced
6 fluorescence) [*Thornton et al.*, 2000], PAN (PI: Singh, electron-capture gas chromatography)
7 [*Singh et al.*, 2000, 2007], HNO_3 and H_2O_2 (PI: Wennberg, chemical ionization mass
8 spectrometer) [*Crounse et al.*, 2006], total alkyl- and hydroxyalkyl-nitrates (AN, PI: Cohen,
9 thermal dissociation - laser induced fluorescence) [*Day et al.*, 2002; *Cleary et al.*, 2005] and
10 CH_2O (PI: Fried, TDLAS) [*Roller et al.*, 2006, and references therein; *Fried et al.*, 2006].
11 Observations shown from the NOAA WP-3D are: ozone (PI: Ryerson, chemiluminescence)
12 [*Ryerson et al.*, 2003], CO (PI: Holloway, vacuum UV fluorescence) [*Holloway et al.*, 2000],
13 isoprene, methylvinyl ketone + methacrolein (MVK+MACR), and monoterpenes (PIs: de Gouw
14 and Warneke, PTR-MS) [*de Gouw et al.*, 2003, 2006], and PAN (PI: Flocke, thermal
15 dissociation-chemical ionization mass spectrometry) [*Slusher et al.*, 2004].



1



2

3 **Figure 2.** Budgets of isoprene nitrates (ONITR+XNITR+ISOPNO3) in the eastern United States
 4 (24-52°N, 62.5-97.5°W) boundary layer (below 800 hPa) during July 2004 for each model

- 1 simulation (Table 2). Production of isoprene nitrates occurs from terpenes (pinene), methylvinyl
- 2 ketone and methacrolein (MACR), and from isoprene reactions with NO_3 (NO_3) and OH (ISOP).
- 3 Loss occurs via photolysis and vertical diffusion ($h\nu + \text{DIF}$), reaction with OH (OH) and ozone
- 4 (O_3), wet deposition (WD), advection (ADV), convection (CNV), and dry deposition (DD).

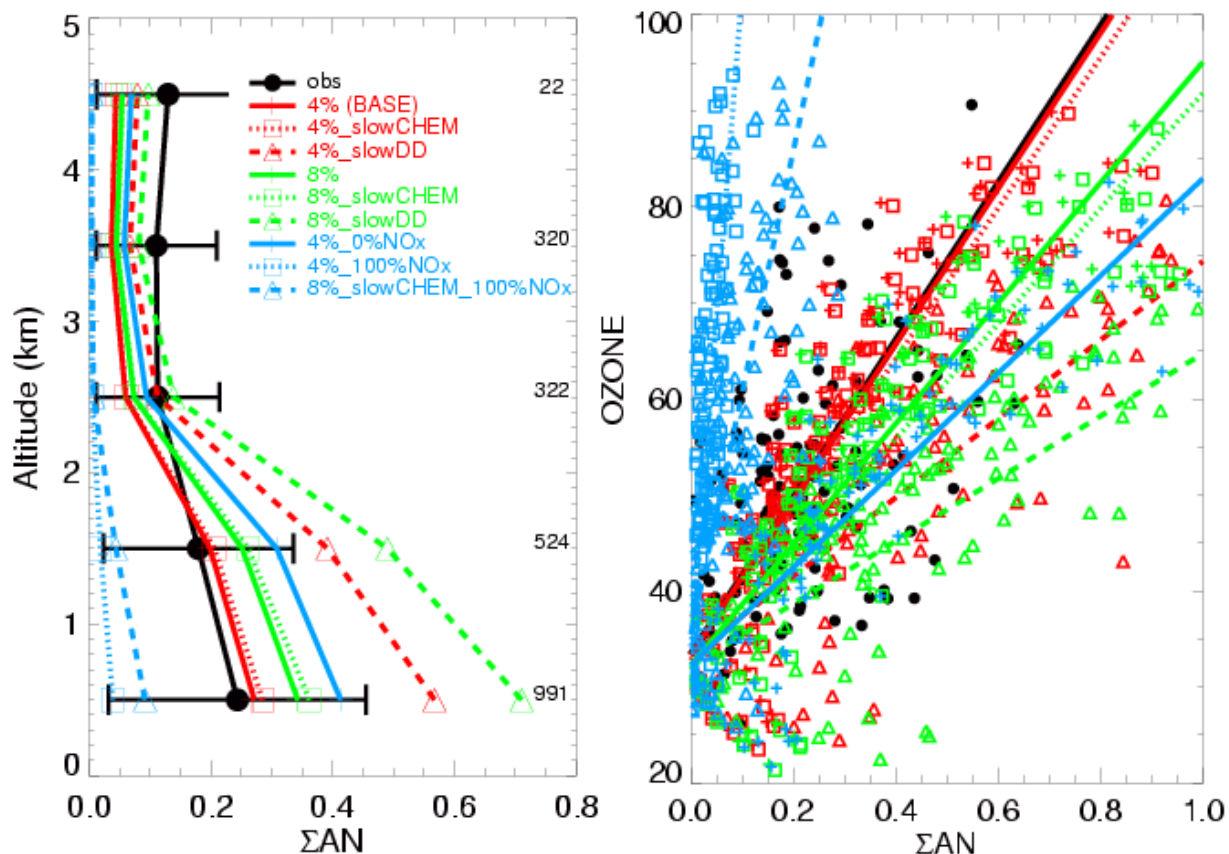


Figure 3. Mean ICARTT vertical profile of the sum of all alkyl nitrates (ΣAN) from observations (black, standard deviations indicated by horizontal bars) and model (colored by simulation as shown in legend; see also Table 2) from all DC-8 flights (left). Correlation plot of ozone versus ΣAN and reduced major axis regression line from observations (black points and line) and model (colored points and lines) for daytime (1500-2300 UTC) DC-8 data over the eastern United States (24-52°N, 62.5-97.5°W) (right). Hourly model results are sampled at the locations of the 1-minute observations. In the ozone- ΣAN correlation plot, 1-minute data points for each flight have been averaged onto the model grid.

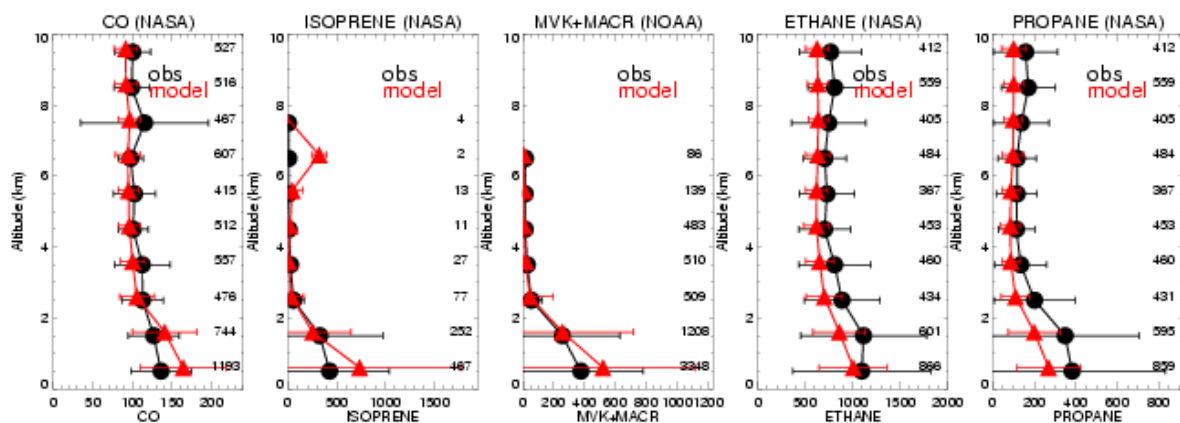


Figure 4. Mean ICARTT vertical profiles of CO, isoprene, methylvinyl ketone + methacrolein, ethane, and propane from observations on the NASA DC-8 and NOAA WP-3D (black, standard deviations indicated by horizontal bars) and model sampled along the appropriate flight tracks (red). Hourly model results are sampled at the locations of the 1-minute observations.